Whole body adhesion: hierarchical, directional and distributed control of adhesive forces for a climbing robot

Sangbae Kim, Matthew Spenko, Salomon Trujillo, Barrett Heyneman, Virgilio Mattoli, Mark R. Cutkosky
Center for Design Research
Stanford University
Stanford, CA 94305-2232, USA
contact: sangbae@stanford.edu

***Abstract*— We describe the design and control of a new bio-inspired climbing robot designed to scale smooth vertical surfaces using anisotropic frictional materials. The robot, called Stickybot, draws its inspiration from geckos and other climbing lizards and employs similar compliance and force control strategies to climb smooth vertical surfaces including glass, tile and plastic panels. Foremost among the design features embodied in Stickybot are multiple levels of compliance, at length scales ranging from centimeters to micrometers, to allow the robot to conform to surfaces and maintain large real areas of contact so that adhesive forces can support it. Structures within the feet ensure even stress distributions over each toe and facilitate engagement and disengagement of the adhesive materials. A force control strategy works in conjunction with the anisotropic adhesive materials to obtain sufficient levels of friction and adhesion for climbing with low attachment and detachment forces.**

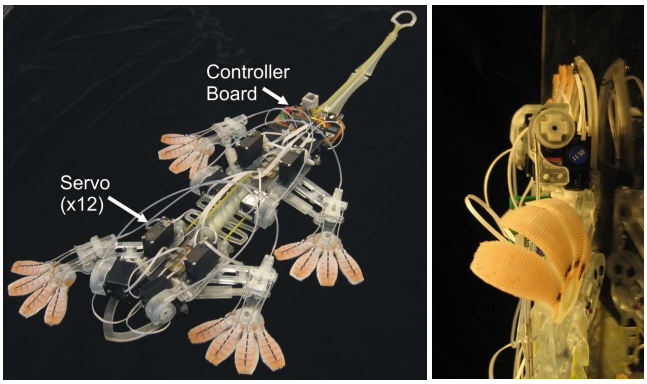

Fig. 1. Left: Stickybot, a new bio-inspired robot capable of climbing smooth surfaces. Right: a sideview of Stickybot climbing vertical glass.

I. Introduction

Robots capable of climbing vertical surfaces would be useful for disaster relief, surveillance, and maintenance applications. Various robots have used suction [13], [27] and magnets [5], [24] for climbing smooth surfaces. A controlled vortex that creates negative aerodynamic lift has also been demonstrated [22]; however, it requires substantial power and generates noise even when stationary. Microspines, drawing inspiration from insects and spiders, have been used to climb rough surfaces such as brick and concrete [1], [18].

For climbing on a range of vertical surfaces from smooth glass to rough stucco, various animals including insects, spiders, tree frogs and geckos employ wet or dry adhesion. The impressive climbing performance of these creatures has lead to a number of robots that employ adhesives for climbing. Sticky adhesives have the disadvantage that they quickly become dirty and lose adhesion [8], [14], [20]. Another disadvantage is that the adhesive requires relatively high forces for attachment and detachment. Some researchers have circumvented this problem by using clever spoked-wheel designs that allow the detachment forces at a receding point of contact to provide the necessary attachment force at the next [8].

To overcome the issue of fouling, there has been a trend toward developing "dry adhesives" which generally have a higher elastic modulus than PSAs and rely on van der Waals forces between arrays of microscopic features and the substrate for adhesion. These have been modeled on the adhesive properties of geckos [4]. In other work, climbing robots have used elastomeric microstructured tape or elastomeric pads that attract dirt after repeated use but, in contrast to PSAs, can be cleaned with water and reused [7], [21].

As feature sizes grow smaller, increasingly stiff and hydrophobic materials can be used while still obtaining sufficient real areas of contact for van der Waals forces to provide useful levels of adhesion [9], [16]. The result is an adhesive that resists dirt accumulation. Various groups are working on synthetic dry adhesives [15], [19], [26]. Currently, no single solution generates high adhesion, attaches with low preload, and is rugged and self-cleaning; however, there is steady progress in each of these directions.

This paper argues that three interconnected design principles are essential for a legged robot to climb and maneuver on vertical surfaces using dry adhesion:

1) hierarchical compliance for conforming at centimeter, millimeter, and micrometer scales;
2) directional adhesives so that the robot can control adhesion by controlling shear; and
3) distributed force control that works with compliance and anisotropy to achieve stability.

This paper reviews these principles in the gecko and describes how they are implemented on Stickybot, a new bio-inspired quadruped robot designed to climb smooth vertical surfaces (See Figure 1). Experimental results of Stickybot climbing glass are included. The paper concludes with discussion of ongoing work to improve the reliability and

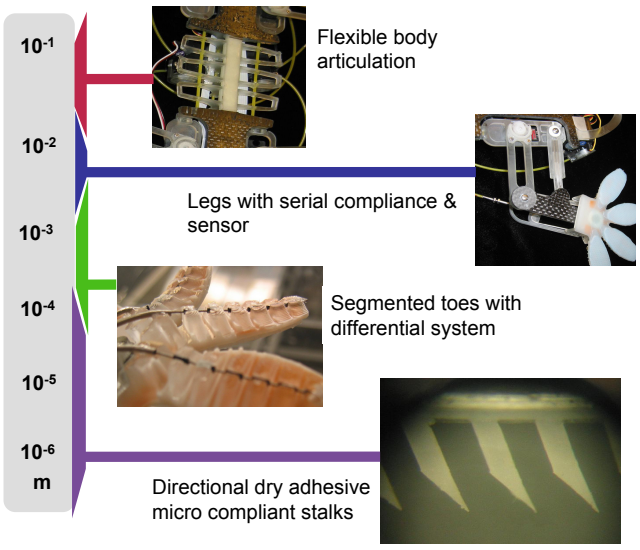

Fig. 2. Illustration of Stickybot's hierarchical compliance over a range of length scales.

performance of Stickybot. A companion paper [17] describes the detailed design and fabrication of the adhesive patches that Stickybot uses.

II. Design Principles for Climbing with Dry Adhesion

This section describes how the principles of hierarchical compliance, anisotropic adhesion and friction, and distributed force control, are applied to Stickybot.

A. Hierarchical Compliance

Climbing with van der Waals forces requires intimate contact because the forces scale as A/d^3 where A is the Hammacher constant and d is the local separation between two surfaces. For particular material combinations the Hammacher constant can vary by as much as a factor of 4 [25]. However, reducing the separation distance has a much greater effect, making it essential to comply to surfaces at all length scales above tens of nanometers.

Natural materials, and many man-made materials such as concrete, have an approximately fractal surface topography. As a result, surface features such as protrusions or indentations can be found at many length scales, from centimeters to fractions of micrometers. Consequently, a general purpose solution for dry adhesion must involve conformability over similar length scales.

In the gecko, the flex of the body and limbs allows for conformation at the centimeter scale. The feet are divided into several toes that can conform independently at a scale of several millimeters. The bottom surfaces of toes are covered with lamellae that conform at the millimeter scale. The lamellae are composed of many individual setae, each of which acts as a spring-loaded beam that provides conformability at the 1-50 micrometer scale. The tips of the setae are divided into hundreds of spatulae that provide conformability at the $<$500 nanometer scale. The consequence of the gecko's hierarchical system of compliances is that it can achieve levels of adhesion of over 500 KPa on a wide variety of surfaces from glass to rough rock and can support its entire weight from just one toe [4].

To enable Stickybot to climb a variety of surfaces from glass to corrugated siding an analogous, albeit much less sophisticated, hierarchy of compliances has been employed (Figure 2). The body of Stickybot is a highly compliant under-actuated system comprised of 12 servos and 38 degrees of freedom. The torso and limbs are created via Shape Deposition Manufacturing [23], [6] using two different grades of polyurethane (Innovative Polymers: 72 Shore-DC and 20 Shore-A hardness).

The stiffest and strongest components of Stickybot are the upper and lower torso and the forelimbs, which are reinforced with carbon fiber. The central part of the body represents a compromise between sufficient compliance to conform to gently curved surfaces and sufficient stiffness so that maximum normal forces of approximately +/- 1N can be applied at the feet without producing excessive body torsion. Additionally, the spine structure at the center of body has the ability to provide body articulation for greater maneuverability in the future.

Each limb is equipped with four segmented toes comprised of two grades of polyurethane and reinforced with embedded synthetic cloth fiber (Figure 3). A single servomotor actuates the toes using a double-rocker linkage and steel cables in metal sleeves (Figure 4) that allow the toes to attach independently to objects with a minimum radius of curvature of 5cm. The toes can also peel backward in a motion approximating the digital hyperextension that geckos use to detach their feet with very little force.

Assuming an approximately uniform toe width, the toe's cable profile is calculated to achieve a uniform stress distribution when the toes are deployed on flat surfaces (Figure 5). The sum of the forces in the y direction is given as:

$$T\sin\theta - T\sin(\theta+\delta\theta) + F_n = 0 \qquad (1)$$

where T is the force acting along the cable, θ is the angle of the cable with respect to the horizontal, and F_n is the normal

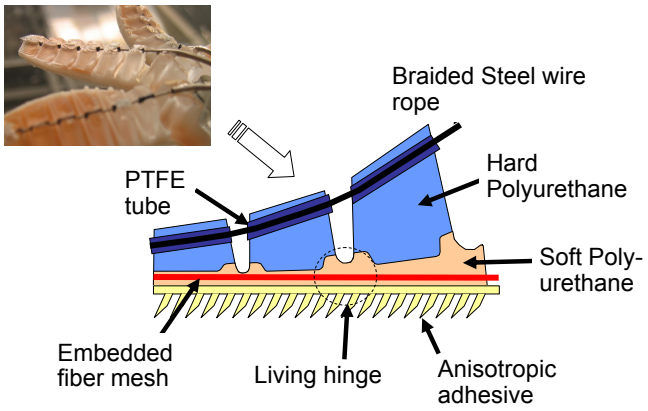

Fig. 3. Schematic of cross section view of Stickybot toe fabricated via Shape Deposition Manufacturing.

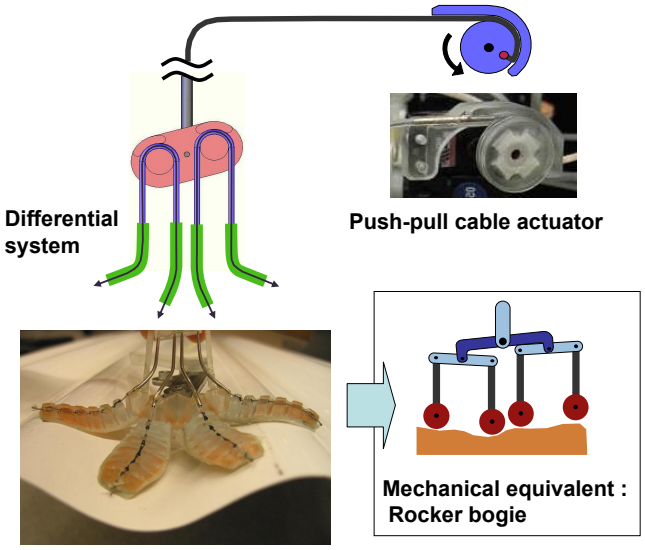

Fig. 4. Two stage differential system actuated by a single push pull actuator. It facilitates conformation on uneven surfaces and distributes the contact forces among four toes.

force acting on the bottom of the toe. To ensure uniform attachment of the foot, a constant pressure on the bottom of the toe is desired:

$$\frac{T\left(\sin\left(\theta+d\theta\right)-\sin\theta\right)}{dx}=\frac{F_n}{dx}=\sigma \tag{2}$$

Expanding the term $\sin\left(\theta+d\theta\right)$ and assuming that $d\theta$ is small such that $\cos d\theta=1$ and $\sin d\theta=d\theta$ yields:

$$\cos\theta d\theta=\frac{\sigma}{T}dx \tag{3}$$

Integrating both sides and solving for θ gives:

$$\theta=\arcsin\left(\frac{\sigma x}{T}\right) \tag{4}$$

The slope of the cable profile is thus:

$$\frac{dy}{dx}=\tan\left(\arcsin\left(\frac{\sigma x}{T}\right)\right) \tag{5}$$

Integrating with respect to x yields the profile of the cable:

$$y\left(x\right)=-\frac{T}{\sigma}\sqrt{1-\left(\frac{\sigma x}{T}\right)^2} \tag{6}$$

which is simply a circular arc with radius T/σ.

At the finest scale, the contact surfaces of the feet are equipped with synthetic adhesive materials (Figure 3). To date, the best results have been obtained with arrays of small, asymmetric elastomeric features as shown in Figure 6. The arrays are made by micromolding with a soft (Shore 20-A) urethane polymer [17]. This structure allows anisotropic compliance that is essential for the directional adhesive behavior addressed in following section. Continued research involves alternative methods of fabrication with stiffer materials and smaller feature sizes to allow for additional levels of hierarchy.

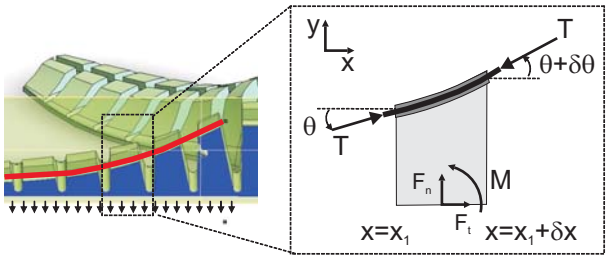

Fig. 5. Details of nomenclature used to calculate cable profile of the toes.

B. Anisotropic Friction and Adhesion

As mentioned in the previous section, geckos can achieve levels of adhesion of over 500 KPa over areas of several square millimeters. However, adhesion only occurs if the lamellae and setae are loaded in the proper direction (inward from the distal toward the proximal region of the toes) [2]. As the setae first contact the surface there is a transient positive normal force due to their elasticity. Shortly thereafter, the tips of the setae grab the surface and the normal force becomes tensile. The maximum pull-off force is related directly to the amount of tangential force present. Conversely, if the toes are brought into contact while moving from the proximal toward the tip regions (i.e., pushing along the toes rather than pulling) no adhesion is observed and the tangential force is limited by a coefficient of friction. The tangential and normal forces contact limits can be modeled as:

$$\begin{array}{c} F_N \geq -\frac{1}{\mu}F_T \\ F_N \geq -\tan\left(\alpha*\right)F_T \end{array} \quad \begin{cases} F_T < 0 \\ 0 \leq F_T \leq F_{\max} \end{cases} \tag{7}$$

where $\alpha*$ is the critical peel angle [2], μ is the coefficient of friction, F_T is tangential (shear) load, taken positive when pulling inward, and F_N is the normal force, taken positive when compressive. The limit, F_{max}, is a function of the maximum shear load that the gecko or robot can apply, the material strength, and the shear strength of the contact interface. Thus, the adhesion increases proportionally with the applied tangential force. This feature, coupled with the gecko's hierarchical compliance, allows it to adhere to

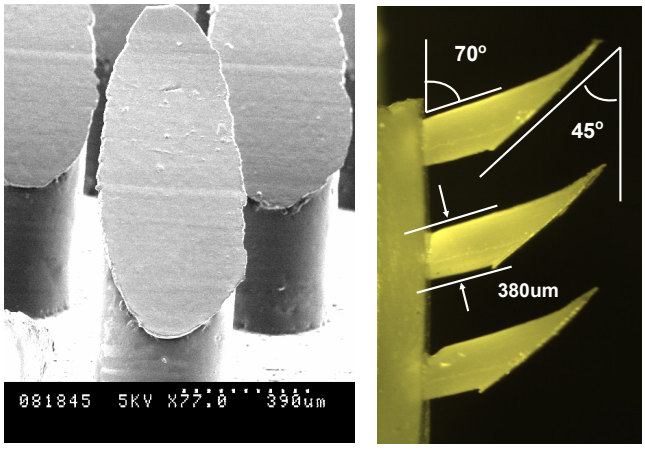

Fig. 6. Anisotropic hairs comprised of 20 Shore-A polyurethane. Hairs measure 380 μm in diameter at the base. The base angle is 20° and the tip angle is 45°.

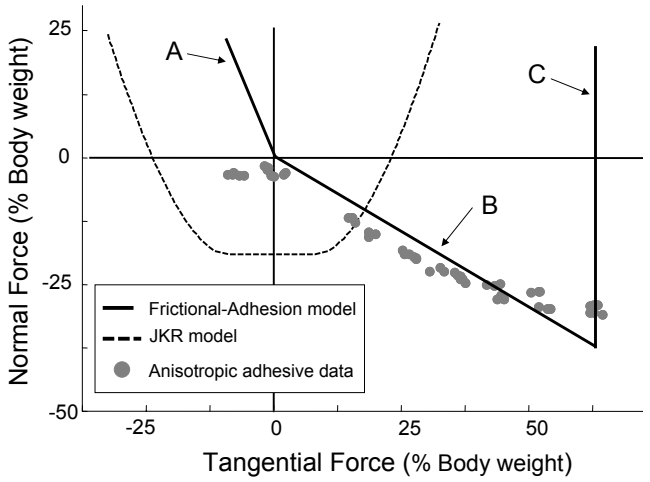

Fig. 7. Comparison of the frictional-adhesion model [2] and the Johnson-Kendall-Roberts (JKR) model [11] with pull off force data from a single toe of Stickybot's anisotropic patches (513 stalks). (A) When dragged against the preferred direction, the anisotropic patch exhibits negligible adhesion, although it sustains greater tangential force than would be expected from Coulomb friction when the normal force is zero. (B) When dragged in the preferred direction, the anisotropic patch demonstrates adhesion proportional to the shear force, albeit with saturation at the highest levels (unlike gecko setae). (C) The frictional-adhesion model has an upper shear force limit. In comparison, the JKR model shows the typical behavior of an isotropic elastic material with adhesion.

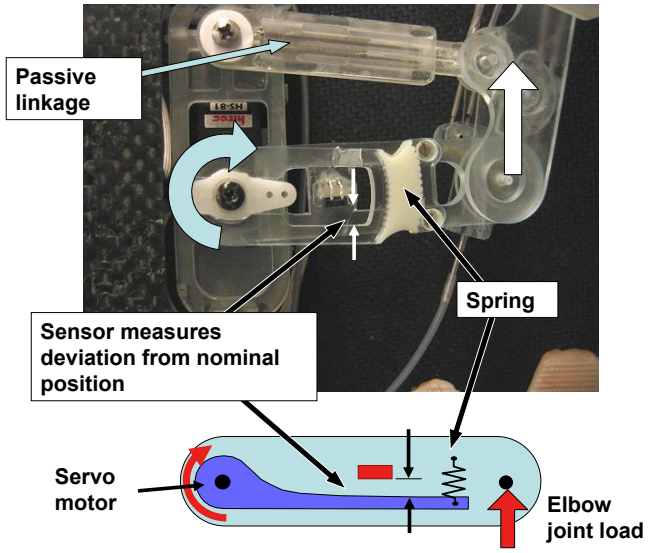

Fig. 8. Traction force sensor measuring deviation of serial compliance at shoulder joint.

surfaces without applying a significant preload. This is beneficial since any preload can cause a gecko (or robot) to push itself away from the wall. Additionally, by decreasing the shear load, the gecko is able to release its foot from the wall gracefully, with zero normal force. Figure 7 illustrates the directional adhesion model in comparison to the commonly used isotropic Johnson-Kendall-Roberts (JKR) model for elastomers [11]. In contrast to the frictional adhesion model, the JKR model's limit surface does not intersect the origin. Instead, the maximum adhesion force is obtained when there is zero shear force, which is much less useful for climbing on vertical surfaces. Moreover, detachment requires a high normal force unless a high tangential force is also present.

Stickybot's anisotropic adhesive patches approximately follow the frictional-adhesion model [2] as shown by data if Figure 7. Evidence of low preload and detachment forces is presented in the Results section. Early versions of Stickybot used isotropic adhesive patches comprised of polyurethane (Innovative Polymers Shore 20A) or Sorbothane®. The large detachment forces caused undesirable force transients to propagate throughout the body and prematurely detach the other feet. Reliable climbing was not obtained until the anisotropic features were added. The anistropic patches also work in conjunction with Stickybot's underactuated limbs: because the patches essentially self-adhere when they are pulled in shear, the toes automatically align themselves to surfaces to maximize the contact area.

C. Distributed Force Control

Distributed force control ensures that stresses are uniformly distributed over the toes and that undesirable force transients and accompanying oscillations are avoided. At the toe level, embedded flexible fabric (Figure 3) allows the feet to obtain a more uniform shear loading over the toes. Together, the fabric and the cable "tendons" provide a load path that routes tangential forces from the toes to the ankles without producing undesired bending moments or stretching that would cause crack propagation and premature peeling at one edge of a toe. At the foot level, ankle compliance and a two stage differential mechanism balance normal forces among toes. At the body level, Stickybot utilizes force control to manage the tangential forces at the feet. This allows Stickybot to maintain dynamic equilibrium as well as increase or decrease the allowable adhesion force (as dictated by the frictional-adhesion model).

Unlike a walking or running quadruped, a climbing quadruped must pay continuous attention to the control of internal forces whenever feet are in contact with the climbing surface. Also, it is important to unload feet in the tangential direction (to relax any built-up forces and accompanying elastic deflections) immediately before lift-off so as to prevent transient forces and associated oscillations that could cause other feet to lose their grip. In geckos, it has been observed that there are virtually no noticeable transient forces as feet make and break contact. Attachment and liftoff are smooth, low-force events [3]. In Stickybot, as in geckos, the combination of toe peeling (digital hyperextension) and directional adhesion are used to minimize detachment forces.

To achieve smooth engagement and disengagement and control its internal forces, Stickybot uses force feedback coupled with a stiffness controller. Stickybot has force sensors located on its shoulder joints (Figure 8) that measure the deflection of an elastomeric spring via a ratiometric Hall effect sensor (Honeywell: SS495A). In addition to providing an estimate of the force, the compliance helps to distribute forces among the limbs such that excessive internal forces do not occur and lead to contact failure.

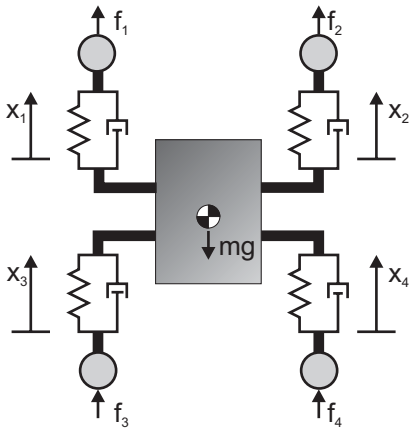

Fig. 9. Schematic used to generate values for the grasp matrix

Stickybot is controlled using a single master microcontroller (PIC18F4520) connected to four slave microcontrollers (PIC12F683) using an I^2C bus. The master microcontroller produces twelve pulse-width-modulation signals to control each servo separately. Each slave microcontroller reads and digitizes data from the force sensors and transmits it to the master microcontroller.

Stickybot's controller must consider limb coordination, which presents two different and sometimes contradictory goals: force balancing and leg phasing. In addition, certain stable limb combinations must be in contact with the climbing surface at all times (i.e., Stickybot must use either a diagonal trot or tripedal crawl). To achieve this, three separate control laws for four different stages of leg motion (stance, detachment, flight, attachment) are implemented.

1) Stance Controller: During stance, the controller implements force balancing using a grasp-space stiffness controller [12]. Since Stickybot uses servomotors that only accept position commands, the stiffness control law is given as:

$$\mathbf{x_{cmd}}(s) = \mathbf{x_{ff}}(s) + \left(k_P + \frac{k_I}{s}\right)\mathbf{C}\left(\mathbf{f_s}(s) - \mathbf{f_d}(s)\right) \quad (8)$$

where $\mathbf{x_{cmd}}$ is a vector comprised of the stroke servo commanded positions, $\mathbf{x_{ff}}$ is the feed forward position command, k_P and k_I are the proportional and integral gains respectively, $\mathbf{C}$ is the compliance matrix, $\mathbf{f_s}$ is a vector comprised of sensed traction forces from each leg, and $\mathbf{f_d}$ is a vector of desired traction forces. While a diagonal compliance matrix would result in independent leg control, during stance $\mathbf{C}$ is defined as:

$$\mathbf{C} = \mathbf{G}^{-1}\mathbf{C_0}\mathbf{G} \quad (9)$$

where $\mathbf{C_0}$ is a diagonal gain matrix chosen such that $\mathbf{C_0} \neq \mathbf{I}$ and $\mathbf{G}$ is the grasp matrix given as:

$$\mathbf{G} = \frac{1}{2}\begin{bmatrix} 1 & 1 & 1 & 1 \\ 1 & -1 & 1 & -1 \\ 1 & 1 & -1 & -1 \\ 1 & -1 & -1 & 1 \end{bmatrix} \quad (10)$$

The grasp matrix is comprised of four independent "grasp modes." The first row in $\mathbf{G}$ is formed by summing the grasp forces in the Y-direction (Figure 9). The second row is produced by summing the moments about the center of mass. The third and fourth rows are chosen such that $\mathbf{G}$ is orthogonal. The chosen values correspond to a fore-aft coupling and a diagonal coupling of the legs respectively. The implementation of stiffness control in grasp space creates a framework for force distribution. By increasing the compliances of all but the total-traction mode, the robot will evenly distribute the forces between feet and achieve force balance while remaining stiff to other variations in loading.

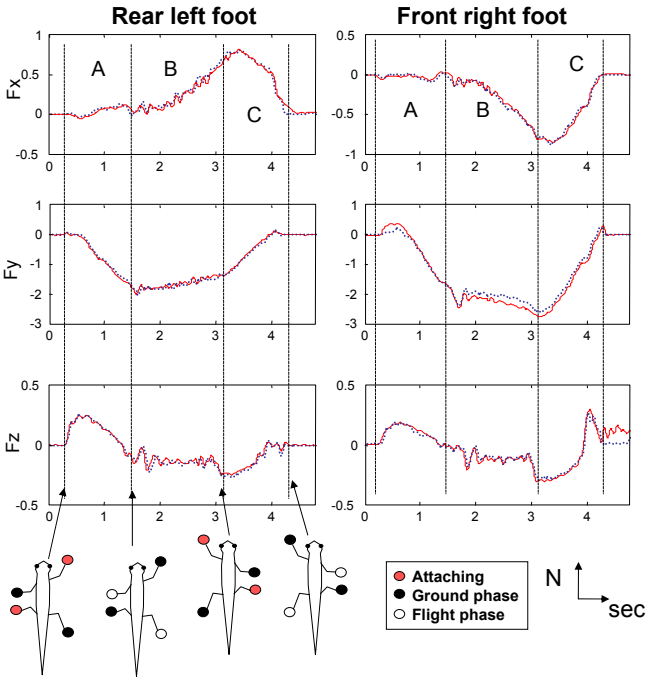

Fig. 10. Force plate data of rear left foot (left) and front right foot (right) of Stickybot climbing with a 6s period at a speed of 1.5 cm/s. Data filtered at 10Hz. Two successive runs are shown to illustrate repeatability.

2) Attachment and Detachment Controller: This controller is identical to the stance controller except that $\mathbf{C} = \mathbf{I}$, which allows each leg to act independently.

3) Flight Controller: During flight, the controller performs phase adjustments, which effectively keeps the legs close to a predefined gait. The flight controller is inspired by [10] and defined as:

$$x_{cmd\_i}(s) = \frac{v_{ff}}{s} + k\left(\phi_i - \frac{\phi_{i+1} + \phi_{i-1}}{2}\right) \quad (11)$$

where v_{ff} is a feed forward velocity, k is a proportional gain, ϕ_i is the phase angle along a nominal leg trajectory, $\phi \in [0, 1]$, and i is the leg detachment order, $i = 1 \ldots 4$.

III. Results

Stickybot is capable of climbing a variety of surfaces at $90\,\mathrm{deg}$ including glass, glossy ceramic tile, acrylic, and polished granite at speeds up to 4.0 cm/s (0.12 body-lengths/s, excluding the tail). The maximum speed of Stickybot on level ground is 24cm/s and is limited by the speed of its actuators (Table I).

Figure 10 presents force plate data of Stickybot climbing vertical glass. The left side shows data from the rear left foot and the right side displays data from the front right foot. Forces are in N and time in seconds. Data from two successive runs are shown to give an indication of the typical repeatability.

Section A (0 to 1.5 seconds) represents the preloading and flexing of the foot. There is almost no force in the lateral (X) direction during preload. The traction force (- Y) is increasing. Although each foot would ideally engage with negligible normal force, there is a small amount of positive normal force during engagement. Weight transfer between diagonal pairs also occurs during section A.

Section B represents the ground stroke phase. There are equal and opposite forces in the X direction for the front right and rear left feet, indicating that the legs are pulling in toward the body. This helps stabilize the body and is similar to the lateral forces exhibited in geckos (and in contrast to the *outward* lateral forces observed in small running animals such as lizards and insects) [3]. The Y-direction shows relatively steady traction force, and the Z-direction indicates adhesion on both the front and rear feet. Note that this differs from gecko data, in which the rear feet exhibit positive normal force [3]. This is due to the fact that Stickybot uses its tail to prevent the body from pitching back, and geckos use their rear feet.

In section C Stickybot releases the feet both by reducing the traction force (Y) and by peeling (utilizing digital hyperextension). Both the front and rear feet exhibit low detachment forces in the Z-direction, especially the rear foot. We note also that the transition between B and C is accompanied by a temporary increase in adhesion (-Z force) and subsequent decrease as the opposite diagonal feet come into engagement.

TABLE I

PHYSICAL PARAMETERS FOR *Stickybot*

Body size	600 x 200 x 60 mm (excluding cables)
Body mass	370 g (including batteries and servo circuitry)
Maximum speed	4.0 cm/s (0.05 bodylength/s)
Servo motors	Hitec HB65 x 8 Hs81 x 4
Batteries	lithium polymer x2 (3.7 V, 480 mAh per pack)

IV. CONCLUSIONS AND FUTURE WORK

Taking cues from geckos, Stickybot uses three main principles to climb smooth surfaces. First, it employs *hierarchical compliance* that conforms at levels ranging from the micrometer to centimeter scale. Second, Stickybot takes advantage of *anisotropic adhesion* that allows it to smoothly engage and disengage from the surface by controlling the traction force. This prevents large disengagement forces from propagating throughout the body and allows the feet to adhere themselves to surfaces when loaded in shear. Interestingly, the motion strategy for engaging adhesives is similar to that used for microspines [1]. Third, Stickybot employs *force control* that works in conjunction with the body compliance and adhesive anisotropic patches to control the traction forces in the feet.

The introduction of better adhesive structures with improved hierarchical compliances will allow Stickybot to climb rougher surfaces and yield longer climbs with an increased resistance to becoming dirty. These improvements may also permit the climbing of overhanging surfaces. Other improvements include improved force control and more attention to the gait and control of internal forces. Additional sensors in the feet should allow the robot to detect when good or poor contact has been made, which will improve the reliability of climbing on varying surfaces. Additional degrees of freedom in the body should allow the robot to master vertical-horizontal transitions and other discontinuities. Once the climbing technology is understood, the ability to climb smooth surfaces will be integrated into the RiSE family of robots in an attempt to design a machine capable of climbing a wide variety of man-made and natural surfaces using a combination of adhesion and microspines [18].

ACKNOWLEDGEMENTS

We thank Jonathan Karpick, Sanjay Dastoor, Arthur McClung, and for their help in circuit board fabrication, coding, and gait generation in support of Stickybot. The development of Stickybot is supported by the DARPA BioDynotics program. Matthew Spenko is supported by the Intelligence Community Postdoctoral Fellow Program.

REFERENCES

[1] A. Asbeck, S. Kim, M. Cutkosky, W. Provancher, and M. Lanzetta. Scaling hard vertical surfaces with compliant microspine arrays. *International Journal of Robotics Research*, 2006.

[2] K. Autumn, A. Dittmore, D. Santos, M. Spenko, and M. Cutkosky. Frictional adhesion: a new angle on gecko attachment. *J Exp Biol*, 209(18):3569–3579, 2006.

[3] K. Autumn, S. T. Hsieh, D. M. Dudek, J. Chen, C. Chitaphan, and R. J. Full. Dynamics of geckos running vertically. *J Exp Biol*, 209(2):260–272, 2006.

[4] K. Autumn, M. Sitti, Y. Liang, A. Peattie, W. Hansen, S. Sponberg, T. Kenny, R. Fearing, J. Israelachvili, and R. Full. Evidence for van der waals adhesion in gecko setae. *Proceedings of the National Academy of Sciences of the United States of America*, 99(19):12252–12256, 2002.

[5] C. Balaguer, A. Gimenez, J. Pastor, V. Padron, and C. Abderrahim. A climbing autonomous robot for inspection applications in 3d complex environments. *Robotica*, 18(3):287–297, 2000.

[6] M. Binnard and M. Cutkosky. A design by composition approach for layered manufacturing. *ASME Transactions, Journal of Mechanical Design*, 122(1), 2000.

[7] K. Daltorio, S. Gorb, A. Peressadko, A. Horchler, R. Ritzmann, and R. Quinn. A robot that climbs walls using micro-structured polymer feet. In *International Conference on Climbing and Walking Robots (CLAWAR)*, 2005.

[8] K. Daltorio, A. Horchler, S. Gorb, R. Ritzmann, and R. Quinn. A small wall-walking robot with compliant, adhesive feet. In *International Conference on Intelligent Robots and Systems*, 2005.

[9] H. Gao, X. Wang, H. Yao, S. Gorb, and E. Arzt. Mechanics of hierarchical adhesion structures of geckos. *Mechanics of Materials*, 37:275–285, 2005.

[10] G.C. Haynes and A. Rizzi. Gait regulation and feedback on a robotic climbing hexapod. In *Proceedings of Robotics: Science and Systems*, Philadelphia, 2006.

[11] K.L. Johnson, K. Kendall, and A.D. Roberts. Surface energy and the contact of elastic solids. *Proceedings of the Royal Society A: Mathematical, Physical and Engineering Sciences*, 324(1558):301–313, 1971.

[12] J. Kerr and B. Roth. Analysis of multifingered hands. *The International Journal of Robotics Research*, 4(4):3–17, 1986.

[13] G. La Rosa, M. Messina, G. Muscato, and R. Sinatra. A lowcost lightweight climbing robot for the inspection of vertical surfaces. *Mechatronics*, 12(1):71–96, 2002.
[14] P. Menzel and F. D'Aluisio. *Robo Sapiens*. MIT Press, 2000.
[15] M. Northen and K. Turner. A batch fabricated biomimetic dry adhesive. *Nanotechnology*, 16:1159–1166, 2005.
[16] A. Peressadko and S.N. Gorb. When less is more: experimental evidence for tenacity enhancement by division of contact area. *Journal of Adhesion*, 80(4):247–261, 2004.
[17] D. Santos, S. Kim, M. Spenko, A. Parness, and M. Cutkosky. Directional adhesive structures for controlled climbing on smooth vertical surfaces. In *IEEE ICRA*, Rome, Italy, 2007. Submitted.
[18] A. Saunders, D. Goldman, R. Full, and M. Buehler. The rise climbing robot: body and leg design. In *SPIE Unmanned Systems Technology VII*, volume 6230, Orlando, FL, 2006.
[19] M. Sitti and R. Fearing. Synthetic gecko foot-hair micro/nano-structures as dry adhesives. *Journal of Adhesion Science and Technology*, 17(8):1055, 2003.
[20] M. Sitti and R. Fearing. Synthetic gecko foot-hair micro/nano-structures for future wall climbing robots. In *International Conference on Robotics and Automation*, 2003.
[21] O. Unver, A. Uneri, A. Aydemir, and M. Sitti. Geckobot: a gecko inspired climbing robot using elastomer adhesives. In *IEEE International Conference on Robotics and Automation*, pages 2329–2335, Orlando, FL, 2006.
[22] vortex. www.vortexhc.com, 2006.
[23] L. E. Weiss, R. Merz, F. Prinz, G. Neplotnik, P. Padmanabhan, L. Schultz, and K. Ramaswami. Shape deposition manufacturing of heterogenous structures. *Journal of Manufacturing Systems*, 16(4):239–248, 1997.
[24] Z. Xu and P. Ma. A wall-climbing robot for labeling scale of oil tank's volume. *Robotica*, 20(2):203–207, 2002.
[25] H. Yoshizawa, Y. Chen, and J. Israelachvili. Fundamental mechanisms of interfacial friction. 1. relation between adhesion and friction. *Journal of Physical Chemistry*, 97:4128–4140, 1993.
[26] Y. Zhao, T. Tong, L. Delzeit, A. Kashani, M. Meyyapan, and A. Majumdar. Interfacial energy and strength of multiwalled-carbon-nanotube-based dry adhesive. *Journal of Vacuum Science and Technology B*, 2006.
[27] J. Zhu, D. Sun, and S.K. Tso. Development of a tracked climbing robot. *Journal of Intelligent and Robotic Systems*, 35(4):427–444, 2002.